



HAL
open science

Is anisotropic propagation of polarized molecular distribution the common mechanism of swirling patterns of planar cell polarization?

Hao Zhu

► **To cite this version:**

Hao Zhu. Is anisotropic propagation of polarized molecular distribution the common mechanism of swirling patterns of planar cell polarization?. *Journal of Theoretical Biology*, 2009, 256 (3), pp.315. 10.1016/j.jtbi.2008.08.029 . hal-00554506

HAL Id: hal-00554506

<https://hal.science/hal-00554506>

Submitted on 11 Jan 2011

HAL is a multi-disciplinary open access archive for the deposit and dissemination of scientific research documents, whether they are published or not. The documents may come from teaching and research institutions in France or abroad, or from public or private research centers.

L'archive ouverte pluridisciplinaire **HAL**, est destinée au dépôt et à la diffusion de documents scientifiques de niveau recherche, publiés ou non, émanant des établissements d'enseignement et de recherche français ou étrangers, des laboratoires publics ou privés.

Author's Accepted Manuscript

Is anisotropic propagation of polarized molecular distribution the common mechanism of swirling patterns of planar cell polarization?

Hao Zhu

PII: S0022-5193(08)00462-1
DOI: doi:10.1016/j.jtbi.2008.08.029
Reference: YJTBI 5276



www.elsevier.com/locate/jtbi

To appear in: *Journal of Theoretical Biology*

Received date: 1 February 2008
Revised date: 28 August 2008
Accepted date: 28 August 2008

Cite this article as: Hao Zhu, Is anisotropic propagation of polarized molecular distribution the common mechanism of swirling patterns of planar cell polarization?, *Journal of Theoretical Biology* (2008), doi:[10.1016/j.jtbi.2008.08.029](https://doi.org/10.1016/j.jtbi.2008.08.029)

This is a PDF file of an unedited manuscript that has been accepted for publication. As a service to our customers we are providing this early version of the manuscript. The manuscript will undergo copyediting, typesetting, and review of the resulting galley proof before it is published in its final citable form. Please note that during the production process errors may be discovered which could affect the content, and all legal disclaimers that apply to the journal pertain.

24 molecular distribution may be the common mechanism of swirling patterns caused by different
25 mutations. It also suggests that at the cell level, as at the molecular level, a simple mechanism can
26 generate complex and diverse cellular patterns in different molecular contexts. The similarity between
27 the induced polarization and its propagation both in the epithelial cells and the dielectric molecules
28 also interestingly suggests some commonalities between pattern formation in the biological and
29 physical systems.

30 **Keywords: anisotropy, dipole, planar cell polarity, propagation, swirling pattern**

31

32 INTRODUCTION

33 From flies to vertebrates during embryogenesis, epithelial cells develop both apicobasal polarity (AP)
34 perpendicular to the tissue surface and planar cell polarity (PCP) along the tissue surface. AP
35 determines the apical and basal sides of cells and PCP aligns cells with their neighbors. As PCP is
36 involved in diverse tissue patterning, distinct mutation phenotypes are widely observed in different
37 animal tissues (Adler, 2002; Klein and Mlodzik, 2005; Zallen, 2007). Of particular interest are
38 domineering nonautonomy (Vinson and Adler 1987) and swirling patterns (Gubb and Garcia-Bellido,
39 1982). The former refers to the mutations affecting cell polarization not only in a mutant clone but also
40 in the nearby wild-type cells; the latter refers to whorls and tufts of hairs and bristles in the wing and
41 the abdomen of *Drosophila* and in the skin of vertebrates (Adler et al., 1998; Casal et al., 2002; Wang
42 et al., 2006). Considerable biological experiments and mathematical modeling have been made to
43 understand domineering nonautonomy. Despite that the detailed signaling processes are still
44 controversial (Lawrence et al., 2007), most studies suggest that the molecular interactions within and
45 between the cells are responsible for the propagation of polarized molecular distribution, thus, the

46 observed domineering nonautonomy (Tree et al., 2002b; Amonlirdviman et al., 2005; Le Garrec et al.,
47 2006). The swirling patterns, in contrast, have been less investigated and remain elusive.

48

49 PCP in different tissues undergoes three stages of molecular signaling conducted by the proteins in
50 three layers (Tree et al., 2002a). In the first stage, the interactions among proteins in the top layer,
51 principally Four-jointed (Fj), Dachshous (Ds), and Fat (Ft), generate a global directional cue to guide
52 cell polarization (Adler et al., 1998; Zeidler et al., 1999; Casal et al., 2002; Rawls et al., 2002; Yang et
53 al., 2002; Cho and Irvine, 2004). In the second stage, under the global cue the interactions among
54 proteins in the middle layer, including Frizzled (Fz), Dishevelled (Dsh), Vang-gogh (Vang), Prickle
55 (Pk), and Flamingo (Fmi), make proteins develop polarized distributions in the cells (Vinson et al.,
56 1989; Tayler et al., 1998; Usui et al., 1999; Krasnow et al., 1995; Tree et al., 2002b; Lawrence et al.,
57 2004). In the third stage, the interactions among a set of tissue-specific proteins in the bottom layer
58 generate tissue-specific phenotypes, such as hair directions in the vertebrate skin and *Drosophila* wing
59 and ommatidia rotation in the *Drosophila* eye. Interestingly, while mutations in *fz* and *vang* in the
60 middle layer usually cause domineering nonautonomy, mutations in genes in both the top and middle
61 layers widely lead to swirling patterns. The underlying mechanisms, however, are unclear.

62

63 As swirling patterns are observed in tissues with mutations in the genes controlling directional cue
64 generation, it is suggested that they are caused by PCP signaling in cells without a cue or with a
65 random cue (Ma et al., 2003). However, rather than being purely random, these patterns show
66 noticeable features. Especially, the hair directions are globally swirling and locally aligned, for which a
67 satisfactory explanation is absent. With a qualitative model, by applying a computational (cellular
68 automata) rule to all of the cells such that each cell iteratively updates its direction on the vector sum

69 of its nearest neighbors' directions, Wang et al. produced different swirling patterns under different
70 initial conditions (Wang et al., 2006). Since hair directions become very regular at the steady state,
71 they propose that local cell interactions initiate a self-organizing process making PCP locally aligned.
72 This explanation, to some extent, justifies the observed global features, but accounts inadequately for
73 the obvious differences between swirling patterns and the wild-type phenotype. Besides, swirling
74 patterns caused by the mutations in *fz* , *dsh* , *inturnd (in)* , and *pk* , which function during the second
75 stage of PCP to amplify and propagate cell polarization, were not addressed (Wang et al., 2006).
76 Recently, it is reported that Fz and Pk, the two key components in the second stage PCP signaling, are
77 required for the hexagonal packing of wing epithelial cells (Classen et al., 2005). Since the hexagonal
78 packing process overlaps in time with the second stage PCP signaling, PCP propagation in unpacked or
79 poorly packed cells may affect PCP patterning significantly.

80

81 We are currently interested in swirling patterns in the *Drosophila* wing. Although the details of
82 molecular signaling have not been fully revealed, polarized molecular distributions have been well
83 characterized. Driven by the directional cue, Fz moves distally and Vang moves proximally in the cell,
84 forming a dipolar Fz/Vang distribution. This distribution is amplified by the intracellular Fz/Dsh and
85 Vang/Pk signaling, which results in a dipolar Dsh/Pk distribution. The two dipolar distributions are
86 stabilized by the cadherin Fmi between the cell and its neighbors (Adler, 2002; Klein and Mlodzik,
87 2005). During the second stage of PCP, the wing epithelial cells also undergo hexagonal packing.
88 Initially, cells are in different shapes—tetragon, pentagon, hexagon, heptagon, and octagon. After
89 hexagonal packing, about 80% of cells are hexagons.

90

91 Molecular signaling and cellular patterning contribute to tissue development at two levels.
92 Experimental studies have revealed some common mechanisms of molecular signaling, including
93 lateral inhibition, positive and negative feedback, and the cell fate determination by morphogen
94 gradient. However, the question of whether there exist common mechanisms of cellular patterning has
95 not been adequately addressed. It is important to reveal these mechanisms and their relationships with
96 molecular signaling. Here, instead of investigating detailed PCP signaling at biochemical reaction level
97 (Amonlirdviman et al., 2005; Le Garrec et al., 2006), we use modeling and simulations to investigate
98 the mechanisms and characteristics of cellular patterning that generate swirling patterns. This study
99 addresses *why* and *how* mutations in the genes in different layers and affecting different aspects of PCP
100 can all lead to swirling patterns. Our exploration complements the experimentally addressed questions
101 such as ‘*what molecules take what functions in what interactions.*’

102
103 Cell polarization is guided by the directional cue, modified by intercellular signaling, and amplified by
104 intracellular signaling. Analogous to the dipolar distribution of positive and negative charges in a
105 dielectric molecule, the dipolar distribution of Fz/Vang in an epithelial cell induces polarization in the
106 neighboring cells. Hence, a polarizing epithelial cell is modeled as a polarizing dielectric molecule (Fig.
107 1AB). With this conceptually clear and simple model, following questions have been addressed: (i)
108 how do defects in the four aspects, i.e., directional cue, hexagonal packing, intercellular signaling, and
109 intracellular signaling, affect PCP; (ii) is there any common mechanism behind various swirling
110 patterns caused by the defects in these aspects; and (iii) what are the conditions required for generating
111 typical swirling patterns? Simulations show that, compared with the defects in directional cue, the
112 defects in hexagonal packing affect PCP less; nevertheless, both make the propagation of PCP
113 anisotropic. The anisotropic propagation makes cell polarization globally disorganized but locally

114 aligned. In a mutant clone without a cue or with a random cue, the propagation from normal cells into
115 mutant cells can be affected by both the cell neighborhood and the clone shape. Moreover, as long as
116 boundaries exist in cells due to defects or differences in any of the mentioned aspects (e.g., packed and
117 unpacked cells, differently packed cells, and different strength of inter- and intracellular signaling),
118 they may contribute to the anisotropic propagation of PCP. These results suggest the anisotropic
119 propagation of polarized molecular distribution as the common mechanism of swirling patterns caused
120 by mutations in different PCP genes. They also imply that at the cell level, as at the molecular level
121 (Affolter and Mann, 2001), complex and diverse cellular patterning could be accounted for by limited
122 number of mechanisms. These results also reveal an interesting similarity between swirling patterns in
123 PCP and spiral waves in cardiac arrhythmias, caused by anisotropic propagation of molecular signaling
124 and of electric excitations, respectively (Pertsov et al., 1993). Moreover, as polarized dielectric
125 molecules via the van der Waals force cause physical morphogeneses such as gas condensation and
126 polarized epithelial cells via the intercellular molecular binding cause biological morphogeneses such
127 as epithelial patterning, a common principle can be presumed to exist in some biological and physical
128 patterning.

129

130 **METHODS**

131 **Biological aspects.** The model contains a lattice of 50x50 cells in different shapes and orientations in
132 the Cartesian coordinate system. Despite the fact that geometrically a cell has eight surrounding cells,
133 its real interactors (called *neighbors* henceforth) are neighborhood-dependent and dynamically
134 changeable. Since cells connect with each other tightly, the cell neighborhood, shape, and orientation
135 are mutually determined (Fig. 1DE). Of the 23 different cell shapes and orientations, there are 2
136 tetragons, 8 pentagons, 4 hexagons, 8 heptagons, and 1 octagon (Fig. S1A). Compared with the

137 uniform cells with a regular and uniform neighborhood in previous PCP models, diverse and
138 changeable cell shapes and orientations with irregular and changeable neighborhoods greatly help the
139 modeling and simulation of complex patterns.

140

141 Several features of PCP and hexagonal packing in the wing allow the computation to be reasonably
142 simplified. First, perimeter of pentagonal, hexagonal, and heptagonal cells are not significantly
143 different (Classen et al., 2005), thus cells are assumed to have the same perimeter. Second, the
144 junctional material in a cell is distributed symmetrically between neighbors (Classen et al., 2005), thus
145 each cell's membrane (perimeter) is assumed to be equally shared by its neighbors. Third, since the
146 dipolar Fz/Vang distribution induced by intercellular Fz/Vang interaction relies on the shared
147 membrane, but not on the physical distance between the connecting cells, the latter can be assumed
148 equal. Fourth, as the Fz/Vang polarity in a cell shows little impact on the Fz/Vang distribution in
149 neighbors in the axis perpendicular to the Fz/Vang polarity, the impact on the two neighbors can be
150 neglected (Fig. 1AB). Fifth, typically non-existing triangular and enneagonal cells are neglected.
151 Finally, since the cell shape, orientation and cell neighborhood are mutually determined, different
152 neighborhoods are used to represent different cell shapes and orientations.

153

154 **Computing cell polarity.** A cell's polarity P , a vector, is divided into two components P_x and P_y in the
155 X and Y direction. Similarly, its impact E on a neighboring cell at point W is divided into E_x and E_y .
156 The change in P_x/P_y is determined both by modification of P_x/P_y by intercellular signaling, $f(P_x)$ and
157 $f(P_y)$, and by amplification of P_x/P_y by intracellular signaling, $g(P_x)$ and $g(P_y)$, which can be
158 described by

$$159 \quad \frac{\partial P_x}{\partial t} = f(P_x) + g(P_x) \quad (1a)$$

$$160 \quad \frac{\partial P_y}{\partial t} = f(P_y) + g(P_y) \quad (1b)$$

161 According to assumptions 1–3, if a cell has n neighbors, there are $f(P_x) = D \cdot \frac{\sum_{i=1}^n E_{x_i}}{n}$ and

$$162 \quad f(P_y) = D \cdot \frac{\sum_{i=1}^n E_{y_i}}{n}, \text{ with the parameter } D \text{ reflecting the strength of intercellular signaling. As}$$

163 intracellular signaling does not change the cell polarity and molecule transportation, irrespective of
 164 whether it is via biochemical reactions or via microtubules (Shimada et al., 2006), is assumed to be at
 165 the steady state, a constant g is used to reflect the consistent strength of intracellular signaling.

166 Therefore, the change in P_x/P_y can be computed by the two reaction-diffusion style equations

$$167 \quad \frac{\partial P_x}{\partial t} = D \cdot \frac{\sum_{i=1}^n E_{x_i}}{n} + g \cdot P_x \quad (2a)$$

$$168 \quad \frac{\partial P_y}{\partial t} = D \cdot \frac{\sum_{i=1}^n E_{y_i}}{n} + g \cdot P_y \quad (2b)$$

169

170 E_x and E_y are computed in the same way as that of the induced polarization of dielectric molecules. If
 171 a polarized dielectric molecule is on the X-axis and at the origin (Fig. 1C), the X and Y components of
 172 its electric field at point W are (Benedek and Villars, 2000),

$$173 \quad E_x = -\frac{\partial E}{\partial x} = \frac{P}{4\pi\epsilon_0} \frac{1}{r^3} (3\cos^2\theta - 1) \quad (3a)$$

$$174 \quad E_y = -\frac{\partial E}{\partial y} = \frac{P}{4\pi\epsilon_0} \frac{1}{r^3} 3\cos\theta \sin\theta \quad (3b)$$

175 where $P = \sqrt{P_x^2 + P_y^2}$ is the dipole moment and P_x and P_y are its two components (corresponding to
 176 the cell polarity in the x and y directions, respectively), r is the distance between O and W, and θ is the
 177 angle between OX and OW. On the basis of the third assumption, r is not important, we therefore
 178 choose $r = \sqrt[3]{\frac{1}{4\pi\epsilon_0}}$. If the dielectric molecule is not on OX, the X'Y' coordinate system is used to plot
 179 it on OX' and then Ex' and Ey' are computed with Eqn (3ab). As the angle between OX and OX'
 180 is $\beta = \arctan \frac{P_y}{P_x}$ and θ can be easily determined depending on the position of W and $\theta' = \theta - \beta$ can be
 181 calculated. With computed Ex' and Ey' (Fig. 1C), the following coordinates transformations give Ex
 182 and Ey

$$183 \quad Ex = Ex' \cos \beta - Ey' \sin \beta \quad (4a)$$

$$184 \quad Ey = Ex' \sin \beta + Ey' \cos \beta \quad (4b)$$

185
 186 **Initial and boundary conditions, parameter values and numerical solution.** The X and Y component
 187 of the directional cue were $I_x = 0.01$ and $I_y = 0.0$, which were sufficiently small to allow inter- and
 188 intracellular signaling to have ample time to play their roles. To generate a random directional cue
 189 (presumably slightly weaker than the normal cue), the function *random()* was used to generate a pair of
 190 random numbers between 0.0000~0.0099 for I_x and I_y and another pair of random numbers between
 191 0.00~0.99 to determine the sign of I_x and I_y (negative if > 0.5 and positive otherwise). We assume that
 192 Fz/Vang signaling does not affect Ft/Fj/Ds interactions, which are believed to determine the directional
 193 cue (Ma et al., 2003; Yang et al., 2002; Matakatsu and Blair, 2004; Cho and Irvine, 2004; Casal et al.,
 194 2002); thus the cue constantly contributes to PCP in each step. Since the lattice is a small patch of
 195 epithelial cells surrounded by the same epithelial cells, the periodic boundary condition was applied.

196 To determine the value of D/g in Eqn (2ab), a pattern of 85% correct hairs (with the remaining outside
197 the range of correct) produced with randomly distributed 85% of cells hexagonally packed under the
198 normal cue was generated with $D = 0.01$ and $g = 0.012$. As this pattern (referred to as simulated wild-
199 type, SWT) matches the reported wild-type phenotype, 0.01/0.012 was set to D/g . The inter- and
200 intracellular signaling of PCP gradually makes all cells maximally and stably polarized, after which no
201 further polarity change occurs. Since after $P > 10.0$ cell polarity changes little, $P > 10.0$ was chosen to
202 terminate simulation when it occurs in $> 96\%$ cells. Eqn (2ab) was solved with the first-order Euler
203 forward method. Since the ‘diffusion’ term does not cause the convergence problem, a large $dt = 1.0$
204 was used.

205
206 **Parameter sensitivity.** It was checked whether the production of the SWT was sensitive to the value of
207 D and g and the ratio of D/g . When D was halved or g was doubled, the results were better, as
208 expected; when D was doubled or g was halved, the results remained largely normal (Fig. S1BC); and
209 when both D/g were doubled or halved, the changes were reasonably in narrower ranges (Fig. S1DE).
210 These results indicate that the SWT is not produced by a system sensitive to D/g .

211
212 **Measure of correct, aligned, and swirling hairs.** In all results, the strength and direction of cell
213 polarity is indicated by the length and direction of the hair. To decipher simulated phenotypes, correct,
214 aligned, and swirling hairs, abbreviated as *correct*, *aligned*, and *swirling* in the text and legends, are
215 quantitatively defined.

216 *Correct:* If a hair is in the direction $[P_x, P_y]$, if $P_x > 0$ & $|P_y / P_x| < 0.1$, then its direction is correct (this
217 hair is counted as *correct* and marked in dark blue in all figures).

218 *Aligned*: If a hair is in the direction $[Py, Px]$ and its eight neighbors in directions $[Py_i, Px_i]$ ($i = 1$ to 8),

219 if for all eight i there exists $\left| \frac{Py_i}{Px_i} \right| / \left| \frac{Py}{Px} \right| < 2.0$ & $\left| \frac{Py}{Px} \right| / \left| \frac{Py_i}{Px_i} \right| < 2.0$, then the hair is aligned

220 with its neighbors (this hair is counted as *aligned* and marked in azure in all figures).

221 *Swirling*: If a hair is in the direction $[Px, Py]$, then its eight neighbors in directions $[Px_i, Py_i]$ ($i = 1$ to 8)

222 are treated clockwise to count the number of adjacent hair pairs in the clockwise direction,

223 CLOCKWISE, and the number of adjacent hair pairs in the anticlockwise direction,

224 ANTICLOCK. For a hair pair, if the hair directions are in the same quadrant, clockwise/

225 anticlockwise is determined by their slope Py/Px , if the hair directions are in two adjacent

226 quadrants, clockwise/anticlockwise is determined by the quadrant relation, if hair directions

227 are in two disjoint quadrants, clockwise/anticlockwise is undetermined. If $CLOCKWISE -$

228 $ANTICLOCK \geq 6$ or $ANTICLOCK - CLOCKWISE \geq 6$, then this hair's eight neighbors

229 comprise a swirl (all nine cells are counted as *swirling* and marked in red in all figures).

230 Values of *correct*, *aligned*, and *swirling* are given when results are compared or their qualitative

231 features are not distinctive.

232

233 RESULTS

234 Hexagonal packing slightly, but directional cue significantly, determines the normal PCP

235 In the *Drosophila* wing, before hexagonal packing, epithelial cells are about 5% tetragon, 35%

236 pentagon, 44% hexagon, and 16% heptagon, and at the end of hexagonal packing about 80% of cells

237 become hexagon (Classen et al., 2005). Hexagonal packing overlaps in time with Fz coordinated PCP

238 signaling, and at the end of PCP Fz/Vang and Dsh/Pk acquire dipolar distributions in cells. To

239 investigate swirling patterns under various conditions, a pattern of 85% correct hairs produced with

240 85% of cells hexagonally packed under the normal cue was first produced (Fig. 2A, captured at step
241 190, *correct* = 2101). This SWT pattern matches to the observed wild-type PCP. In the following parts,
242 unless specified, “packed” means hexagonally packed cells in the shape 11 (Fig. S1A), “unpacked”
243 means non-hexagonal cells equally in tetragons, pentagons, and heptagons, and “mixed” means the cell
244 population before hexagonal packing. Packed cells, unpacked cells, and mixed cells are randomly
245 distributed.

246
247 In theory, defects in hexagonal packing or in directional cue would affect PCP. To study PCP in poorly
248 packed cells under the normal cue, simulations were made in (i) 50% packed and 50% unpacked cells
249 and (ii) mixed cells. The difference in results is quantitative but not qualitative (Fig. S2A, captured at
250 step 189, *correct* = 1459; Fig. S2B, captured at step 191, *correct* = 1111). To check the impact of
251 hexagonally packed but randomly oriented cells on PCP, hexagons in different orientations were
252 employed to perform the simulations. The results were not better than the PCP simulated in mixed
253 cells (Fig. S2C, captured at step 191, *correct*=910).

254
255 To check the impact of directional cue, two simulations were made in packed and mixed cells under a
256 random cue. Both resulted in highly irregular yet similar patterns. Quantitatively, PCP in mixed cells
257 (Fig. S2D, captured at step 320, *swirling* = 432, *correct* = 76) is worse and slower than in packed cells
258 (Fig. 2B, captured at step 320, *swirling* = 171, *correct* = 55), which is a reasonable result. These results
259 agree with the experimental finding that in the PCP mutant wing defects in hexagonal packing do not
260 much perturb the cell polarity (Classen et al., 2005), thereby highlighting the importance of directional
261 cue.

262

263 Rescue of directional cue, hexagonal packing, intracellular and intercellular signaling

264 To further evaluate the relative importance of hexagonal packing and directional cue, similar to
265 rescuing *fz* function in experiment by restoring *fz* expression at different times (Strutt and Strutt, 2002),
266 packed cells and directional cue were made available at different times in simulations. First, PCP in
267 packed cells under a random cue was simulated, during which the normal cue was restored at step 10
268 (Fig. 3A, captured at step 243) and 50 (Fig. 3B, captured at step 300). The results show that, to
269 produce a largely correct PCP the cue should be rescued at a very early time, and a rescue at a step as
270 late as 50 produced a slower PCP and an irregular pattern qualitatively similar to PCP in packed cells
271 under a random cue (Fig. 2B). Simulations in mixed cells under the normal cue were also made, with
272 cells becoming packed later. It was found that a rescue of hexagonal packing at a step as late as 150
273 was enough to produce a quite normal pattern (Fig. S3A, captured at step 189, *correct* = 1100). These
274 results further support the mentioned conclusion that the hexagonal packing slightly, but directional
275 cue significantly, determines the normal PCP. *In vivo*, the directional cue could affect PCP in two
276 linked ways, via hexagonal packing and via Fz signaling (Strutt and Strutt, 2002; Classen et al., 2005),
277 which might explain its importance. As will be discussed later, under the normal cue and with intact
278 intracellular signaling PCP does not rely much on hexagonal packing, but when intracellular signaling
279 is impaired PCP becomes more sensitive to defects in hexagonal packing.

280

281 To check intracellular signaling under the wild-type condition, i.e., 85% of cells packed under the
282 normal cue, PCP without intracellular signaling and with intracellular signaling being rescued at step
283 150 was simulated (Fig. S3B, captured at step 535, *swirling* = 9 and *correct* = 591; Fig. S3C, captured
284 at step 285, *swirling* = 0 and *correct* = 1580). Although quantitatively the result of PCP without
285 intracellular signaling is worse, hair directions are not recognizably swirling. This indicates that

286 intracellular signaling might not be very important under the normal condition, which agrees with the
287 experimental finding (Strutt and Strutt, 2007).

288

289 While intracellular signaling amplifies polarity within cells, intercellular signaling aligns polarity
290 among cells. To check how they would affect PCP under abnormal conditions, simulations were made
291 (i) in packed cells under a random cue and (ii) in mixed cells under the normal cue. First, two
292 simulations were made under conditions (i) without intercellular signaling and condition (ii) without
293 intracellular signaling, respectively (Fig. S3D, captured at step 336, *swirling* = 315 and *correct* = 68;
294 Fig. S3E, captured at step 346, *swirling* = 0 and *correct* = 811). Note, in the second case the cue was
295 slightly amplified to make PCP in the two cases finish at the same time, and the amplified cue
296 contributed to an improved result (make Fig. S3E better than Fig. S3B). Then, two simulations were
297 made under the conditions (i) intercellular signaling was rescued at the mid-time (step 165) and (ii)
298 intracellular signaling was rescued at the mid-time (step 165), respectively (Fig. S3F, captured at step
299 327, *swirling* = 270 and *correct* = 62; Fig. S3G, captured at step 232, *swirling* = 0 and *correct* = 1010).
300 To complete the comparison, further two simulations were made under the conditions (i) and (ii) with
301 intact inter- and intracellular signaling, respectively (Fig. S3H, captured at step 294, *swirling*=171 and
302 *correct*=58; Fig. S3I, captured at step 160, *swirling*=0 and *correct*=1192). In all these cases, PCP under
303 a random cue (Fig. S3DFH) was worse than PCP under the normal cue (Fig. S3EGI), and the rescue of
304 intra- and intercellular signaling always improved PCP. The comparable improvement of PCP by the
305 rescue of inter- and intracellular signaling under the two conditions may indicate a comparable impact
306 of inter- and intracellular signaling on PCP under abnormal conditions.

307

308 **A graded directional cue could make PCP anomalies position-dependent**

309 Mutations in the genes involved in directional cue generation are found to produce position-dependent
310 instead of random aberrances. In the *ds* mutant wing, hair directions at the distal tip are more regular
311 than those in other areas (Adler et al., 1998), and if nonautonomous *fz* function is impaired, hairs at the
312 distal tip are more tolerant than hairs elsewhere (Strutt and Strutt, 2002). In the eye, the proportion of
313 ommatidia showing dorsoventral inversion in an *fz* clone is also position-dependent—about 5% at the
314 equatorial edge, 15%–25% at the center, and 40%–60% at the polar edge (Strutt and Strutt, 2002). To
315 check whether this position-dependency could be caused by a graded cue, a simulation was made in
316 mixed cells under a graded normal cue (the normal cue + column \times 0.0005). The result is not
317 remarkably different from PCP in mixed cells under the normal cue (Fig. S2B), but quantitatively there
318 are fewer correct hairs in the low cue area and more correct hairs in the high cue area (data not shown).
319 This is because the cells under a higher cue are more resistant to the modification of their polarity by
320 neighbors.

321
322 We speculate that if a graded cue is impaired by gene mutations, then the residual cue gradient would
323 still be graded. To check how such a gradient would affect PCP, a simulation in mixed cells under a
324 graded random cue (the random cue + column \times 0.0005) was made. The result is remarkable (Fig. 4A).
325 On the basis of these results, together with the observed distal-to-proximal Fj gradient in the wing (Ma
326 et al. 2003; Matakatsu and Blair, 2004), equator-to-pole Fj gradient in the eye (Yang et al. 2002), and
327 the opposite Ds gradient in the two tissues (Yang et al., 2002; Cho and Irvine, 2004), a graded cue can
328 be speculated in these tissues, which is higher at the distal end in the wing and at the equator edge in
329 the eye. A graded cue provides a simple and plausible explanation not only for those inexplicable
330 position-dependent PCP anomalies in the *Drosophila* wing and eye (Adler et al., 1998; Strutt and Strutt,
331 2002) but also for the finding that hair formation first starts at the distal end in the wing and the earliest

332 ommatidia rotation happens at the equator part in the eye (Wong and Adler, 1993; Wehrli and
333 Tomlinson, 1995).

334

335 **Large clones with an abnormal cue can produce typical swirling patterns**

336 Swirling patterns caused by mutations in different genes are widely observed, however, typical swirls
337 are rare. By analyzing the typical ones (Adler et al., 1997; Adler et al., 1998; Ma et al., 2003; Simon,
338 2004; Matakatsu and Blair, 2004), we find that they show one or several of the following features: (i)
339 changed molecular distribution (the reversed Fz distribution); (ii) specific mutations in some genes
340 ($ft^{l(2)fd}$ and ds^{UAO71}); (iii) large clone; and (iv) irregular clone boundary. An interesting question is
341 whether these features indicate something in common to the generation of typical swirling patterns.
342 Converting these features into simulation conditions, specifically, assuming that $ft^{l(2)fd}$ would eliminate
343 the cue in cells, we addressed this question by investigating the impact of these conditions (the impact
344 of clone boundary is described in the next section).

345

346 First, if a clone was large, with packed cells under the normal cue outside it and mixed cells without
347 cue inside it, typical swirling patterns were generated (Fig. 5A). Besides irregular and swirling hair
348 directions inside the clone, hair directions in some cells outside the clone were also changed. This
349 result is quite similar to the experimentally observed phenotypes (Ma et al., 2003). Small clones were
350 found to less likely to cause swirls, which is in line with the finding that small errors in PCP can be
351 corrected by signaling from neighboring normal cells (Ma et al., 2003). Some mutations could impair
352 rather than eliminate the cue, which raises the question of whether the no-cue condition is
353 indispensable. To investigate it, a simulation with mixed cells under a random cue inside a clone (a
354 random cue is weaker than the normal cue, see Methods) was performed, which also resulted in typical

355 swirls (Fig. 5B). However, if mixed cells in the clone were under the normal cue, a quite regular
356 pattern was acquired (Fig. 5C). These results indicate that a weak and abnormal cue contributes
357 significantly to the generation of typical swirling patterns. To check if the clone shape matters, a round
358 clone and a square clone under the no-cue condition were examined. The result indicates that the clone
359 shape is not critical (Fig. 5DE). Further, to check the impact of a clone of changed molecular
360 distribution, simulations were made with packed cells under the normal cue. When the cue in the clone
361 was rotated by 90 degrees or reversed (Fig. S6AB), though hair directions within or around the clone
362 were changed and somewhat swirling, typical swirls were absent. These results indicate that the
363 changed molecular distribution would affect hair directions but might not significantly contribute to
364 typical swirling patterns. Finally, to check if typical swirls could be produced in a globally graded cue
365 a simulation was made with mixed cells without cue inside the clone and packed cells under the graded
366 normal cue outside it. The graded cue does not noticeably affect the generation of swirling patterns
367 (Fig. 4B).

368
369 These results together suggest that the identified features indeed indicate something in common to the
370 generation of swirling patterns. Generally, under the normal cue, since PCP proceeds at the normal
371 speed and is constrained in the correct direction, it is resistant to the anisotropic propagation caused by
372 flawed cellular packing, whereas under a weak and abnormal cue, since PCP proceeds slowly and is
373 less or wrongly directionally constrained, it is much affected by the anisotropic propagation caused by
374 flawed cellular packing. This explains the previous findings that PCP in mixed cells under the normal
375 cue is quite regular but in packed cells under the random cue is highly irregular (Fig. S2B; Fig. S3H).
376 If a clone is large, the long-range anisotropic propagation significantly promotes the generation of
377 typical swirls.

378

379 **Clone boundary may specifically affect anisotropic propagation**

380 In simulations with mixed cells inside a clone, the anisotropic propagation of PCP is caused by the
381 irregular cell neighborhood inside the clone and around the clone boundary. To check whether and
382 how clone boundary *per se* would affect PCP, simulations where the cells inside and outside a no-cue
383 clone were packed in two different hexagons were performed. This would avoid the anisotropic
384 propagation in the clone caused by the irregular cell neighborhood. Two swirls were found when the
385 shape 11 cells and shape 12 cells were inside and outside of the clone respectively (Fig. 6A; Fig. S1A);
386 however, no swirl was found in the opposite case (Fig. 6B). A closer observation reveals different
387 cross-boundary PCP propagation in these two cases. In the first case, the cross-boundary propagation
388 in many of the cells inside the clone was perpendicular to the outside cell polarity, rendering
389 subsequent propagation in the clone very anisotropic (Fig. 6A). In the second case, the cross-boundary
390 propagation in many of the cells inside the clone was along, or roughly along, the outside cell polarity,
391 rendering subsequent propagation in the clone quite isotropic (Fig. 6B). These observations indicate
392 that the cell neighborhood at the clone boundary may inherently affect cross-boundary PCP
393 propagation and therefore the intra-clone PCP propagation. To check whether this impact is clone-
394 shape-dependent, two simulations under the same conditions but with a square clone were made. The
395 results indicate that the impact is independent of the clone shapes (Fig. S4AB).

396

397 To check whether irregularity of clone boundary matters, another simulation was made with a slightly
398 more complex clone (Fig. 6C). Although the result contains only one defined swirl, globally hair
399 directions seem more irregular than in a simpler clone (Fig. 6AB). This may help explain the

400 observation that swirling patterns are more often seen in clones with a complex and irregular boundary.
401 A complex clone boundary is likely to make cross-boundary PCP propagation anisotropic.

402

403 **Intracellular and intercellular signaling affects PCP differently**

404 Cell polarity is amplified by intracellular Fz/Dsh and Vang/Pk signaling and modified by intercellular
405 Fz/Vang signaling. A recent study indicates that Fz/Vang conducted intercellular signaling does not
406 require Dsh and Pk and takes place earlier than intracellular signaling (Strutt and Strutt, 2007).

407 However, less is known about the contribution of intracellular signaling. In particular, why mutations
408 in genes involved in intracellular signaling cause swirling patterns is poorly understood. With different
409 values of g/D that reflect different relative strengths of intra- and intercellular signaling, simulations
410 were made to address this question.

411

412 When the g/D ratio was decreased by decreasing g 10 times which weakened the intracellular signaling,
413 PCP under the wild-type condition (85% of cells packed under the normal cue) became slower and
414 more irregular (Fig. 7A, *swirling* = 9 and *correct* = 952). When the g/D ratio was decreased by
415 increasing D 10 times which enhanced the intercellular signaling, PCP became very irregular with
416 multiple swirls (Fig. 7B, *swirling* = 171 and *correct* = 136). These results indicate the importance of
417 intracellular signaling, which is supported by the experiments in vertebrates (Wallingford et al., 2000).

418

419 Many swirling patterns are observed in situations of double mutations. To check the combined impact
420 of impaired directional cue and impaired intracellular signaling, the simulation was made under the
421 condition that outside the clone were packed cells under the normal cue but inside the clone were
422 mixed cells without the directional cue and all cells had a 10 times smaller g . The result, compared

423 with PCP under the same condition except a smaller g (Fig. 5A, *swirling*=72), shows some new
424 features: the swirling pattern inside the clone is severer and the hair directions outside the clone are
425 affected more by cross-boundary PCP propagation (Fig. 7C, *swirling*=117).

426
427 In addition to mutant clones with defects in directional cue and hexagonal packing, there can be mutant
428 clones with defects in inter- or intracellular signaling. To check how clones with impaired intracellular
429 signaling affect PCP, two simulations were made with a clone in which intracellular signaling was 10
430 times weaker ($g=0.0012$). In the case where 70% of cells were packed and 30% of cells unpacked,
431 changes in the hair directions widely occurred in the clone (Fig. 7D); in the case where all cells were
432 packed, changes in the hair directions only occurred at the inner clone boundary (Fig. S5). Simulations
433 showed that the weakened intracellular signaling decreased PCP speed and relatively enhanced the
434 intercellular signaling, and the two effects together enhanced the anisotropic propagation of PCP,
435 making it more sensitive to mutant clones, boundaries in the cells, and defects in hexagonal packing.

436

437 **DISCUSSION AND CONCLUSIONS**

438 **The common mechanism of swirling patterns**

439 Swirling patterns are widely observed in different tissues. Compared with domineering nonautonomy,
440 they are less revealed experimentally as well as theoretically. Swirling patterns caused by mutations in
441 *ft*, *fj*, and *ds* can be explained by miss-guided PCP signaling. However, those caused by mutations in
442 genes such as *pk*, *dsh*, and *in* pose a challenging question (Adler et al., 1997; Adler et al., 1998). In the
443 middle or bottom layer of PCP signaling, these genes take different function in intracellular signaling
444 that interprets and amplifies the directional cue. Though mutations in different genes affect PCP
445 signaling differently, they all cause swirling hair patterns. No elegant explanation has been made to

446 reconcile the disparity at the molecular level and the similarity at the cell level. That different
447 mutations can all lead to swirling patterns implies that some common mechanism above molecular
448 signaling may exist and determine swirling pattern generation. To theoretically unveil the mechanism,
449 analogies between the biological system and some physical systems have been suggested, for example,
450 it is proposed that cellular polarization is similar to the patterning of electron spins in the ferromagnet
451 (Lewis and Davies, 2002; Wang et al., 2006).

452

453 In this study, by comparing the induced polarization of a cell to that of a dielectric molecule, a model
454 covering the major aspects of PCP but neglecting the molecular details of the signaling is built.
455 Simulations that produce typical and atypical swirling patterns under various conditions show how
456 impaired directional cue, poor hexagonal packing, weakened intracellular signaling, irregular clone
457 boundary, and inhomogeneous strength of intercellular signaling affect the propagation of PCP. The
458 results not only explain why mutations in genes in intracellular signaling cause swirling patterns but
459 also indicate that the anisotropic propagation of polarized molecular distribution could be the common
460 mechanism of swirling patterns at the cell level.

461

462 Specifically, simulations suggest that swirling patterns caused by weakened intracellular signaling are
463 due to the defects in cellular packing, which, according to Classen et al. (Classen et al., 2005),
464 normally exist in cells. When intracellular signaling is weakened, the impact of the defects on PCP
465 becomes increased. This also reasonably explains why double mutations, for example, one in a gene
466 controlling directional cue generation and the other in a gene participating in intracellular signaling, is
467 more likely to cause swirling patterns. Since the anisotropic propagation caused by defects in cellular
468 packing differs from the anisotropic propagation caused by impaired directional cue, phenotypically

469 the resulting swirling patterns are different. Those seen in *pk* and *dsh* mutants are closer to those seen
 470 in *fz*, *vang* and *fmi* mutants but different from those seen in *ft* and *ds* mutants. Moreover, in *dsh*, *pk*, *fz*
 471 and *vang* mutants the hairs start at the center of the cell but in *ft* and *ds* mutants they start at the one
 472 side of the cell. Despite these differences, at the cell level the anisotropic propagation of cell
 473 polarization occurs in all of the cases, providing a common mechanism to explain different swirling
 474 patterns.

475

476 **A mathematical note**

477 An interesting relationship can be observed by comparing Eqn (2ab) to the Turing reaction-diffusion
 478 equations:

$$479 \quad \frac{\partial C_1}{\partial t} = f(C_1) + D_1 \nabla^2 C_1 \quad (5a)$$

$$480 \quad \frac{\partial C_2}{\partial t} = f(C_2) + D_2 \nabla^2 C_2 \quad (5b)$$

481 In Eqn (2ab), if $D=0$, P_x/P_y would just be amplified I_x/I_y and the cell polarity would match the cue
 482 direction, and if $f(P_x)_{[i,j]} \neq f(P_x)_{[i\pm m, j\pm n]}$ and $f(P_y)_{[i,j]} \neq f(P_y)_{[i\pm m, j\pm n]}$ ($[i,j]$ is cell position and m ,
 483 $n=0$ or 1), the cell polarity would deviate from the cue direction. In Eqn (5ab), if $D_1=D_2=0$, C_1 and C_2
 484 would evolve into a uniform steady state, if $D_1 \neq D_2$, spatially inhomogeneous patterns would be
 485 generated by diffusion-driven instability (Murray, 1990), and if $D_1 = D_2$ but $\nabla^2_{[i,j]} \neq \nabla^2_{[i\pm m, j\pm n]}$, diffusion-
 486 driven instability would also occur, a situation very close to Eqn (2ab). In the two cases,
 487 inhomogeneous diffusion in the cells and inhomogeneous interaction between the cells are essentially
 488 parallel.

489

490 **A possible sufficient condition for generating typical swirling patterns**

491 As typical swirling patterns are not widely observed in experiments, a question is what are the required
492 conditions for generating them? An analysis of those results with clear swirls reveals that typical swirls
493 often occur in large $ft^{1(2)fd}$ and ds^{UAO71} clones. On the basis of the speculation that mutations like $ft^{1(2)fd}$
494 might eliminate the directional cue in cells, simulations were made with a clone without or with a weak
495 directional cue, and typical swirls were produced. Further investigations into the clone size, clone
496 shape, and clone boundary also reveal their effects on swirling pattern generation. These results
497 indicate that the following conditions may comprise a set of sufficient conditions for the generation of
498 typical swirling patterns in a clone: (i) poorly packed cells to create irregular cell neighborhood, (ii)
499 without a cue or with a weak cue to make cell polarization in random directions or at slow speed, (iii) a
500 large clone size to allow long-range propagation, and (iv) a complex clone boundary to make irregular
501 cross-boundary propagation. These conditions should be verified experimentally, for example, to see
502 whether $ft^{1(2)fd}$ would indeed eliminate the cue and whether a simple clone boundary would be less able
503 to produce typical swirls. Such coupled computational and experimental studies, with predictions and
504 verification, would make PCP better understood.

505

506 **Why do swirling patterns show stereotypical global features?**

507 In contrast to typical swirling patterns, atypical ones (globally swirling but without clear whorls and
508 tufts) are widely observed in varied situations. Moreover, some swirling patterns show highly
509 reproducible and stereotypical global features. So, what makes hair directions stereotypically rather
510 than randomly swirling? The simulations of clone boundary provide an answer. In the situations
511 generating typical or atypical swirling patterns, various boundaries could exist in cells, for example,
512 between wild-type and mutant cells, between packed and unpacked cells, between cells with different
513 cue concentration or direction, and between cells with different intra- and intercellular signaling
514 strength. As revealed by the simulations, these boundaries contribute to the anisotropic propagation of

515 PCP, and the contribution becomes significant if other defects coexist. While an impaired cue or the
516 unpacked cells would make fine-grained anisotropic propagation of PCP, such boundaries would cause
517 coarse-grained anisotropic propagation, which explains globally swirling and locally aligned instead of
518 purely random hair directions. Very likely, they may also explain why some swirling patterns show
519 stereotypical global features and are highly reproducible—some of the boundaries may inherently exist
520 in a tissue, with an insignificant effect under the normal situation but a substantial one under abnormal
521 situations on PCP. The uneven distribution of the 15% unpacked cells (Classen et al., 2005) and the
522 existence of wing veins, for example, are two examples.

523

524 **Can the model explain wider epithelial cell polarization?**

525 The impressive agreement between the simulation results and experimental findings supports modeling
526 a polarizing epithelial cell as a polarizing dipole, which allows the major PCP properties determined by
527 core signaling components to be computationally investigated at the cell level. In addition to the
528 Fz/Vang-based PCP in the epidermis, there are other PCP processes based on molecules such as
529 myosin II and Bazooka and involved in other tissue patterning processes, such as convergent extension
530 and gastrulation (Keller, 2002; Zallen and Wieschaus, 2004; Zallen, 2007). These processes show two
531 features: cell polarization is reversible and the relevant molecules adopt polarized (like Fmi in
532 *Drosophila* wing cells) but not dipolar (like Fz/Vang in *Drosophila* wing cells) distribution. Can the
533 model describe such PCP processes? We note that the proposed analogy between the induced
534 polarization of biological cells and the induced polarization of dielectric molecules and the propagation
535 of the polarization do not require an explicit representation of specific molecules such as Fz/Vang or
536 myosin II/Bazooka and, therefore, do not depend on the polarized distribution of a molecule or the
537 dipolar distribution of a pair of molecules. Thus, other PCP related patterning such as the rosette

538 structure in the *Drosophila* embryo could also be modeled (Blankenship et al., 2006). Actually,
539 hexagonal packing of the wing cells during wing development is thought to be quite similar to the cell
540 shape change during embryonic convergent extension (Classen et al., 2005), and it has been proposed
541 that even at the molecular level PCP in different tissues could follow an essentially common
542 mechanism (Mlodzik, 2002).

543

544 **ACKNOWLEDGMENT**

545 The author thanks Drs. Nick Monk and Markus Owen for helpful discussions and the anonymous
546 reviewer for valuable comments.

547

Accepted manuscript

547

548 **REFERENCES**

- 549 Adler, P.N., Krasnow, R.E. and Liu, J. 1997 Tissue polarity points from cells that have higher Frizzled
550 levels towards cells that have lower Frizzled levels. *Curr. Biol.* 7, 940–949.
- 551 Adler, P.N., Charlton, J., and Liu, J. 1998 Mutations in the cadherin superfamily member gene
552 dachsous cause a tissue polarity phenotype by altering frizzled signaling. *Development* 125, 959–
553 968.
- 554 Adler, P.N. 2002 Planar signaling and morphogenesis in *Drosophila*. *Dev. Cell* 2, 525–535.
- 555 Affolter, M. and Mann, R. 2001 Legs, eyes, or wings - selectors and signals make the difference.
556 *Science* 292, 1080–1081.
- 557 Amonlirdviman, K., Khare, N.A., Tree, D.R.P., Chen, W.S., Axelrod, J.D. and Tomlin, C.J. 2005
558 Mathematical modeling of planar cell polarity to understand domineering nonautonomy. *Science*
559 307, 423–426.
- 560 Blankenship, J.T., Backovic, S.T., Sanny, J.S.P., Weitz, O. and Zallen, J.A. 2006 Multicellular rosette
561 formation links planar cell polarity to tissue morphogenesis. *Dev. Cell* 11, 459–470
- 562 Benedek, G.B. and Villars, F.M.H 2000 Physics with illustrative examples from medicine and biology
563 – Electricity and magnetism. 2nd ed. Springer-Verlag.
- 564 Casal, J., Struhl, G. and Lawrence, P.A. 2002 Developmental compartments and planar polarity in
565 *Drosophila*. *Curr. Biol.* 12, 1189–1198.
- 566 Cho, E. and Irvine, K.D. 2004 Action of fat, four-jointed, dachsous and dachsin in distal-to-proximal wing
567 signaling. *Development* 131, 4489–4500.
- 568 Classen, A-K., Anderson, K.I. Marois, E., and Eaton, S. 2005 Hexagonal packing of *Drosophila* wing
569 epithelial cells by the planar cell polarity pathway. *Dev. Cell* 9, 805–817.

- 570 Gubb, D. and Garcia-Bellido, A. 1982 A genetic analysis of the determination of cuticular polarity
571 during development in *Drosophila melanogaster*. *J. Embryol. Exp. Morphol.* 68, 37–57.
- 572 Keller, R. 2002 Shaping the vertebrate body plan by polarized embryonic cell movements. *Science* 298,
573 1950–1954.
- 574 Klein, T.J. and Mlodzik, M. 2005 Planar cell polarity: an emergent model points in the right direction.
575 *Annu. Rev. Cell Dev. Biol.* 21, 155–176.
- 576 Krasnow, R.E., Wong, L.L. and Adler, P.N. 1995 Dishevelled is a component of the frizzled signaling
577 pathway in *Drosophila*. *Development* 121, 4095–4102.
- 578 Lawrence, P.A., Casal, J. and Struhl, G. 2004 Cell interactions and planar polarity in the abdominal
579 epidermis of *Drosophila*. *Development* 131, 4651–4664.
- 580 Lawrence, P.A., Struhl, G. and Casal, J. 2007 Planar cell polarity: one or two pathways? *Nat. Rev.*
581 *Genet.* 8, 555–563.
- 582 Le Garrec, J.F., Lopez, P. and Kerszberg, M. 2006 Establishment and maintenance of planar epithelial
583 cell polarity by asymmetric cadherin bridges: a computer model. *Dev. Dyn.* 235, 235–246.
- 584 Lewis, J. and Davies, A. 2002 Planar cell polarity in the inner ear: how do hair cells acquire their
585 oriented structure? *J. Neurobiol.* 53, 190–201
- 586 Ma, D., Yang, C., McNeill, H., Simon, M.A. and Axelrod, J.D. 2003 Fidelity in planar cell polarity
587 signaling. *Nature* 421, 543–547.
- 588 Matakatsu, H. and Blair, S.S. 2004 Interactions between Fat and Dachshous and the regulation of planar
589 cell polarity in the *Drosophila* wing. *Development* 131, 3785–3794.
- 590 Mlodzik, M. 2002 Planar cell polarization: do the same mechanisms regulate *Drosophila* tissue
591 polarity and vertebrate gastrulation? *Trends in Genetics.* 18, 564–571.
- 592 Murray, J.D. 1990 Discussion: Turing theory of morphogenesis – Its influence on modeling biological

- 593 pattern and form. *Bull. Math. Biol.* 52, 119–152.
- 594 Pertsov, A.M., Davidenko, J.M., Salomonsz, R., Baxter, W.T., and Jalife, J. 1993 Spiral Waves of
595 excitation underlie reentrant activity in isolated cardiac muscle. *Circ. Res.* 72, 631–650.
- 596 Rawls, A.S., Guinto, J.B., and Wolff, T. 2002 The cadherin Fat and Dachshous regulates dorsal/ventral
597 signaling in the *Drosophila* eye. *Curr. Biol.* 12, 1021–1026.
- 598 Shimada, Y., Yonemura, S., Ohkura, H., Strutt, D. and Uemura, T. 2006 Polarized transport of Frizzled
599 along the planar microtubule arrays in *Drosophila* wing epithelium. *Dev. Cell.* 10, 209–222.
- 600 Simon, M.A. 2004 Planar cell polarity in the *Drosophila* eye is directed by graded Four-jointed and
601 Dachshous expression. *Development* 131, 6175–6184.
- 602 Strutt, H. and Strutt, D. 2002 Nonautonomous planar polarity patterning in *Drosophila*: Dishevelled-
603 independent functions of Frizzled. *Dev. Cell* 3, 851–863.
- 604 Strutt, D. and Strutt, H. 2007 Differential activities of the core planar polarity proteins during
605 *Drosophila* wing patterning. *Dev. Biol.* 302, 181–194.
- 606 Tayler, J., Abramova, N., Charlton, J. and Adler, P.N. 1998 Van Gogh: a new *Drosophila* tissue
607 polarity gene. *Genetics* 150, 199–210.
- 608 Tree, D.R.P., Ma, D. and Axelrod, J.D. 2002 A three-tiered mechanism for regulation of planar cell
609 polarity. *Sem. Cell Dev. Biol.* 13, 217–224.
- 610 Tree, D.R.P., Shulman, J.M., Rousset, R., Scott, M.P., Gubb, D. and Axelrod, J.D. 2002 Prickle
611 mediates feedback amplification to generate asymmetric planar cell polarity signaling. *Cell* 109,
612 371–381.
- 613 Usui, T., Shima, Y., Shimada, Y., Hirano, S., Burgess, R.W., Schwarz, T.L., Takeichi, M. and Uemura,
614 T. 1999 Flamingo, a seven-pass transmembrane cadherin, regulates planar cell polarity under the
615 control of Frizzled. *Cell* 98, 585–595.

- 616 Vinson C.R. and Adler P.N. 1987 Directional non-cell autonomy and the transmission of polarity
617 information by the *frizzled* gene of *Drosophila*. *Nature* 329, 549–551.
- 618 Vinson, C.R., Conover, S. and Adler, N. 1989 A *Drosophila* tissue polarity locus encodes a protein
619 containing seven potential transmembrane domains. *Nature* 338, 263–264.
- 620 Wallingford, J.B., Rowning, B.A., Vogeli, K.M., Rothbacher, U., Fraser, S.E., and Harland, R.M. 2000
621 Dishevelled controls cell polarity during *Xenopus* gastrulation. *Nature* 405, 81–85.
- 622 Wang, Y., Badea, T., and Nathans, J. 2006 Order from dis-order: self-organization in mammalian hair
623 patterning. *Proc. Nat. Acad. Sci.* 103, 19800–19805.
- 624 Wehrli, M. and Tomlinson, A. 1995 Epithelial planar polarity in the developing *Drosophila* eye.
625 *Development* 121, 2451–2459.
- 626 Wong, L.L and Adler, P.N 1993 Tissue polarity genes of *Drosophila* regulate the subcellular location
627 for prehair initiation in pupal wing cells. *J. of Cell Biol.* 123, 209–221.
- 628 Yang, C., Axelrod, J.D. and Simon, M. 2002 Regulation of Frizzled by Fat-like cadherins during
629 planar polarity signaling in the *Drosophila* compound eye. *Cell* 108, 675–688.
- 630 Zeidler, M.P., Perrimon, N., and Strutt, D.I. 1999 The four-jointed gene is required in the *Drosophila*
631 eye for ommatidial polarity specification. *Curr. Biol.* 9, 1363–1372.
- 632 Zallen, JA and Wieschaus, E. 2004 Patterned gene expression directs bipolar planar polarity in
633 *Drosophila*. *Dev. Cell* 6, 343–355.
- 634 Zallen, J.A. 2007 Planar polarity and tissue morphogenesis. *Cell* 129, 1051–1063.

635

636

636

637 **LEGENDS**

638 **Fig. 1 The analogy between the induced polarization of epithelial cells and the induced**
639 **polarization of dielectric molecules.** (A) The dipolar F_z/V_{ang} distribution in a cell and the induced
640 dipolar distribution in its neighbors. (B) The dipolar distribution of positive and negative charges in a
641 dielectric molecule and the induced dipolar distribution in its neighbors. (C) The electric field of a
642 polarized dielectric molecule at the origin. (DE) A pentagonal cell has different neighbors when in
643 different orientations.

644

645 **Fig. 2 PCP under a random cue is highly irregular.** (A) In 85% packed cells under the normal cue
646 the wild-type PCP is produced ($swirling=0$, $correct=2101$). The random distribution of the 85% packed
647 and 15% unpacked cells is shown in Fig. 7. (B) In wholly packed cells under a random cue PCP is
648 irregular with swirls ($swirling=171$, $correct=55$). In all figures, *correct* hairs are indicated by dark blue,
649 *aligned* hairs by azure, and *swirling* hairs by red.

650

651 **Fig. 3 An early rescue of directional cue is required for the normal PCP.** PCP in packed cells
652 under a random cue with the normal cue being rescued at step 10 (A) ($swirling=9$, $correct=865$) and at
653 step 50 (B) ($swirling=9$, $correct=161$).

654

655 **Fig. 4 A graded directional cue makes PCP anomaly graded.** (A) PCP in mixed cells under a
656 graded random cue ($swirling=18$, $aligned=16$, $correct=495$). More changed hair directions, including
657 swirls, occur at the left-side low-cue area. (B) PCP under a graded cue with a clone; outside the clone
658 are packed cells under the normal graded cue and inside the clone are mixed cells without the cue.

659

660 **Fig. 5 A large clone and impaired directional cue are critical for generating typical swirling**

661 **patterns.** Outside the clone are packed cells under the normal cue and inside the clone are mixed cells

662 (A) without the cue, (B) under a random cue, (C) under the normal cue, and (DE) without the cue.

663

664 **Fig. 6 The impact of different clone boundary on PCP.** PCP is in packed cells with a no-cue clone,

665 with (A) the shape 11 cells inside and the shape 12 cells outside the clone, (B) the shape 12 cells inside

666 and the shape 11 cells outside the clone, and (C) the shape 11 cells inside and the shape 12 cells

667 outside a more complex clone.

668

669 **Fig. 7 Changed intra- and intercellular signaling has different impact on PCP.** (A) PCP in 85%

670 packed cells under the normal cue with the 10 times weakened intracellular signaling ($g=0.0012$,

671 $swirling=9$ and $correct=952$). (B) PCP in 85% packed cells under the normal cue and the 10 times

672 enhanced intercellular signaling ($D=0.1$, $swirling=171$ and $correct=136$). Grey color indicates the 15%

673 unpacked cells. Compared with Fig. 2A the weakened intracellular and enhanced intercellular

674 signaling makes hair patterns more irregular. (C) PCP with a clone in a background of 10 times

675 weakened intracellular signaling ($g=0.0012$ in all cells). Outside the clone are packed cells under the

676 normal cue and inside the clone are mixed cells without the cue. Compared with Fig. 5A there are

677 more swirls in the clone and more changed hair directions around the clone. (D) PCP with a clone

678 under the normal cue and in a background of poor hexagonal packing (70% of cells packed and 30% of

679 cells unpacked). Inside the clone is the 10 times weakened intracellular signaling ($g=0.0012$ in clone

680 cells). Compared with the hair directions outside the clone, the weakened intracellular signaling inside

681 the clone makes PCP sensitive to defects in hexagonal packing.

682

683 **Fig. S1 The generation of the simulated wild-type is not sensitive to g/D values.** (A) The 23

684 different cell shapes and orientations. Note that this figure does not accurately reflect that the cell's

685 membrane is equally shared by its neighbors. (BCDE) PCP in 85% packed cells under the normal cue

686 with (B) doubled D ($D=0.02$, $correct=1115$), (C) halved g ($g=0.006$, $correct=1620$), (D) doubled D/g 687 ($D=0.02/g=0.024$, $correct=1654$), and (E) halved D/g ($D=0.005/g=0.006$, $correct=2333$).

688

689 **Fig. S2 Directional cue is more important than hexagonal packing for PCP.** (A) PCP in cells 50%690 packed and 50% unpacked under the normal cue ($correct=1459$). (B) PCP in mixed cells under the691 normal cue ($correct=1111$). (C) PCP in randomly oriented hexagons under the normal cue692 ($correct=910$). (D) PCP in mixed cells under a random cue ($swirling=432$, $correct=76$).

693

694 **Fig. S3 Intra- and intercellular signaling has comparable importance in abnormal situations.**

695 (ABC) PCP under the normal cue (A) in mixed cells with packed cells being rescued at step 150

696 ($swirling=0$, $correct=1100$), (B) in 85% packed cells without intracellular signaling ($swirling=9$ and697 $correct=591$), and (C) in 85% packed cells with intracellular signaling being rescued at step 150698 ($swirling=0$ and $correct=1580$). (DFH) PCP in packed cells under a random cue (D) without699 intercellular signaling ($swirling=315$ and $correct=68$), (F) with intercellular signaling being rescued at700 step 165 ($swirling=270$ and $correct=62$), and (H) with intact intercellular signaling ($swirling=171$ and701 $correct=58$). (EGI) PCP in mixed cells under the normal cue (E) without intracellular signaling702 ($swirling=0$ and $correct=811$), (G) with intracellular signaling being rescued at step 165 ($swirling=0$ 703 and $correct=1010$), and (I) with intact intracellular signaling ($swirling=0$ and $correct=1192$).

704

705 **Fig. S4 The impact of clone boundary on PCP.** PCP in cells packed in two different hexagons inside
706 and outside a clone without the cue. (A) Inside the clone are the shape 11 cells and outside the clone
707 are the shape 12 cells. (B) Inside the clone are the shape 12 cells and outside the clone are the shape 11
708 cells.

709

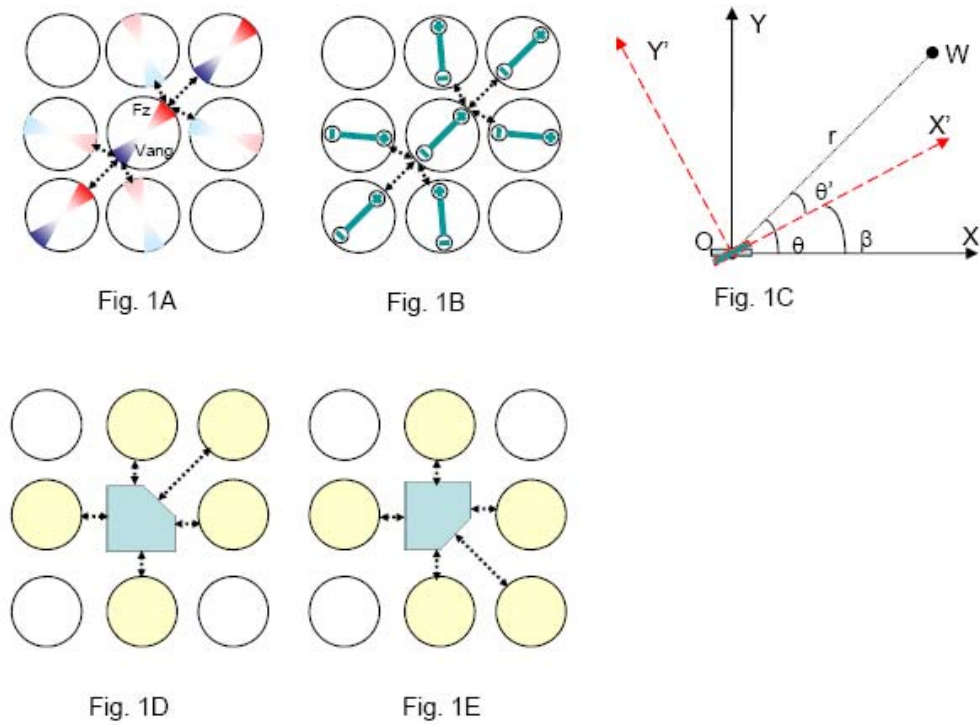
710 **Fig. S5 The impact of inhomogeneous strength of intracellular signaling on PCP.** PCP proceeds in
711 packed cells under the normal cue with a clone inside which $g=0.0012$.

712

713 **Fig. S6 The impact of changed cue direction on PCP.** PCP in packed cells under the normal cue
714 with a clone inside which (A) the cue direction is rotated by 90-degree and (B) the cue direction is
715 reversed.

716

716 Figure 1:



717

718

Accepted

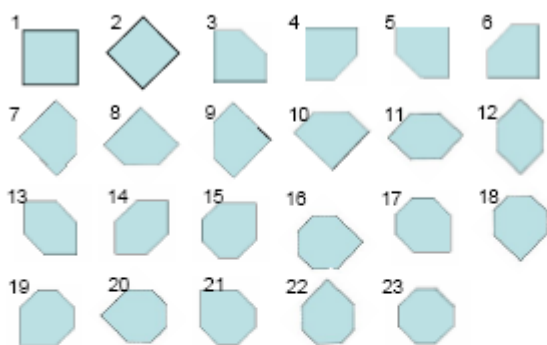


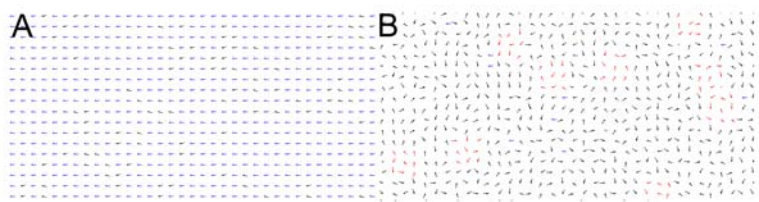
Fig. S1A

718

719

Accepted manuscript

719 Figure 2:

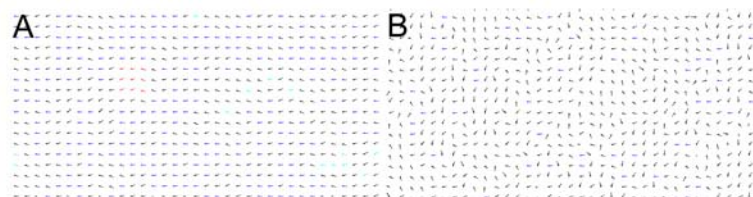


720

721

Accepted manuscript

721 Figure 3:

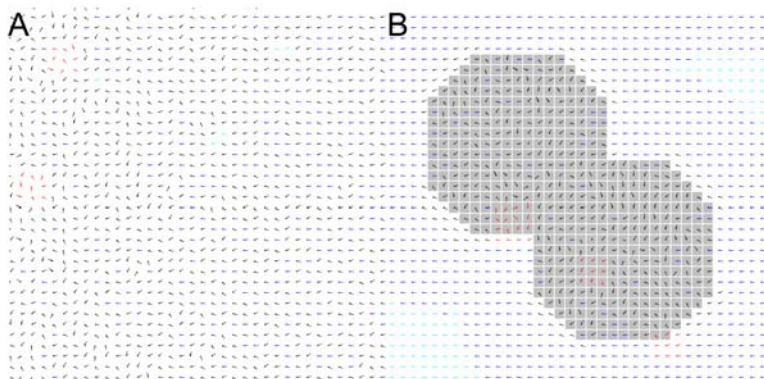


722

723

Accepted manuscript

723 Figure 4:

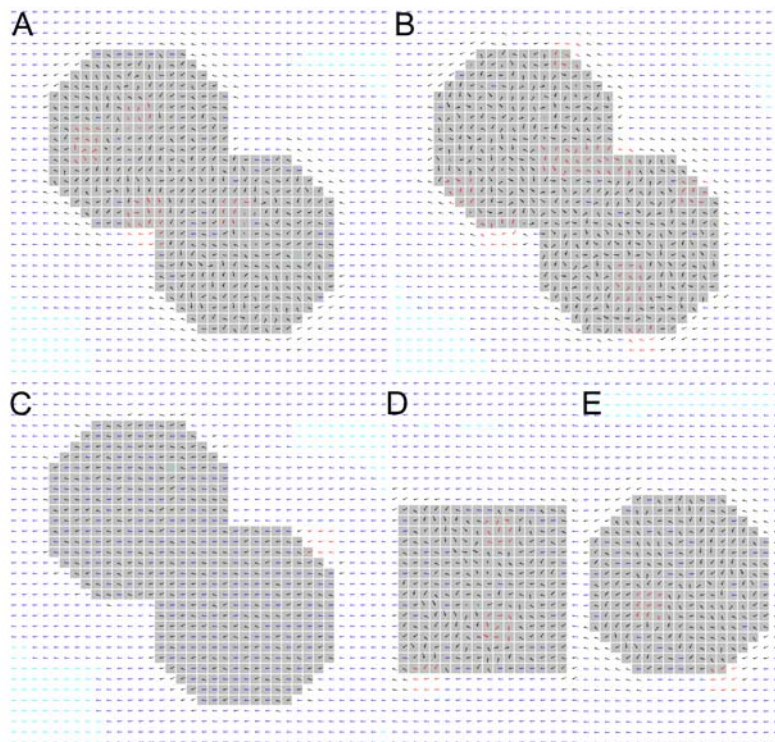


724

725

Accepted manuscript

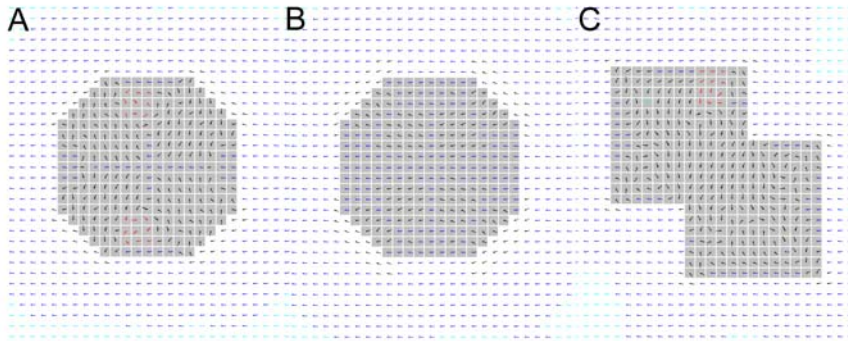
725 Figure 5:



726

727

727 Figure 6:

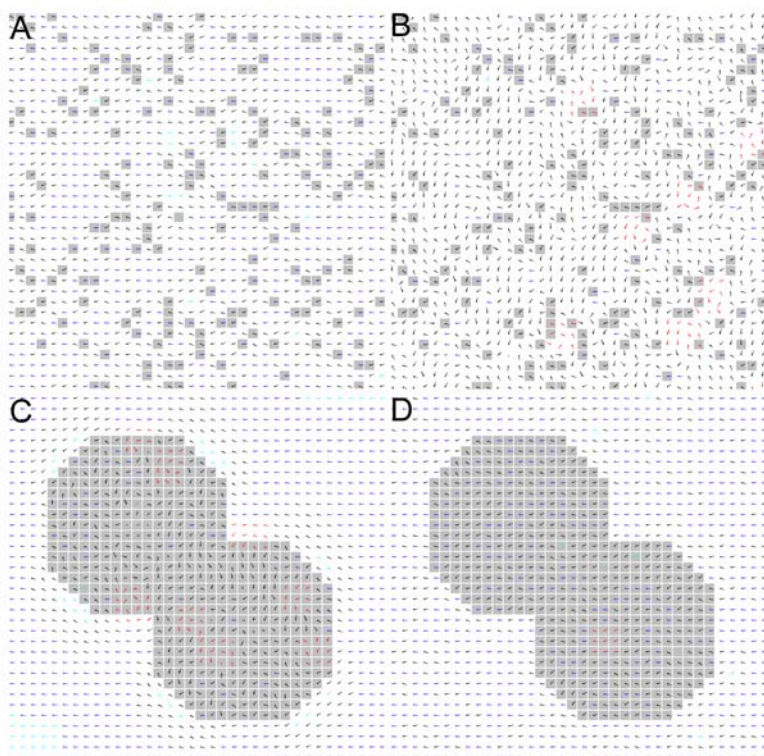


728

729

Accepted manuscript

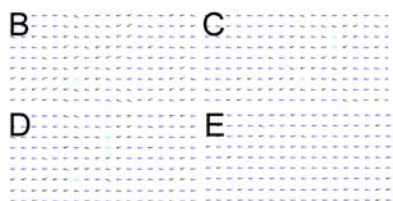
729 Figure 7:



730

731

731 Figure S1:

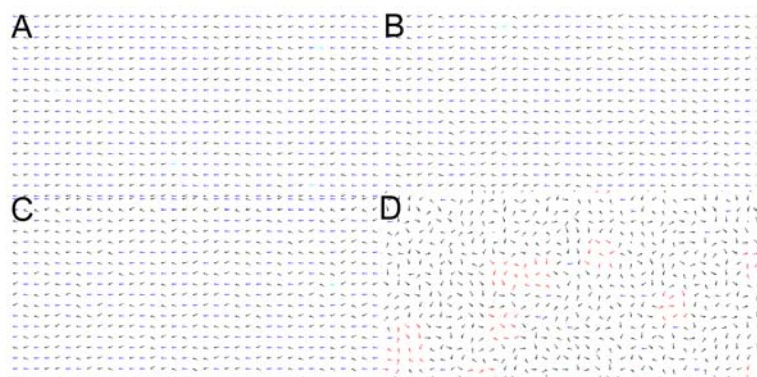


732

733

Accepted manuscript

733 Figure S2:

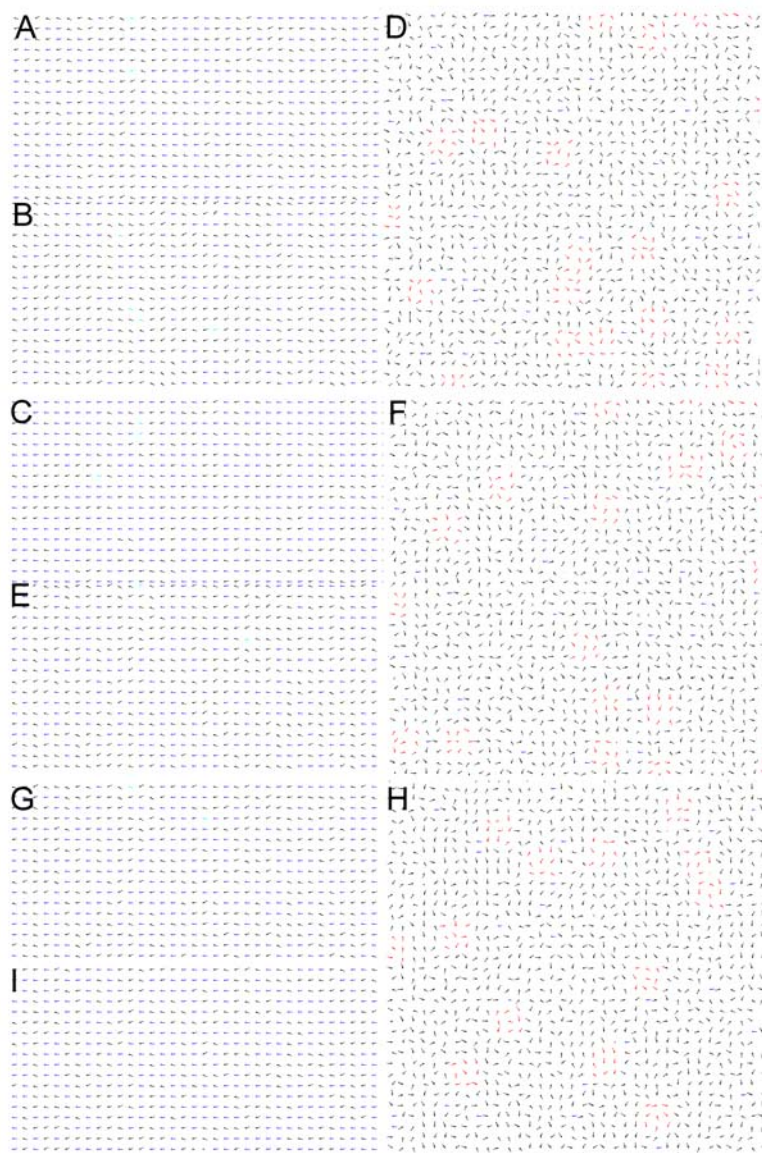


734

735

Accepted manuscript

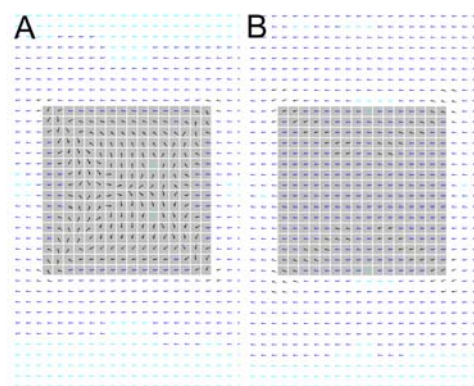
735 Figure S3:



736

737

737 Figurer S4:

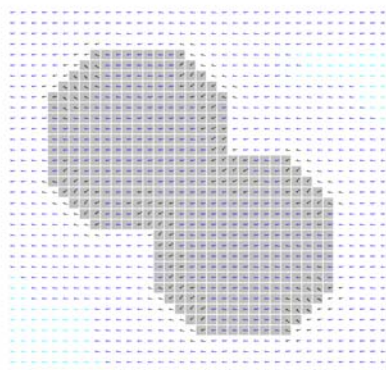


738

739

Accepted manuscript

739 Figure S5:

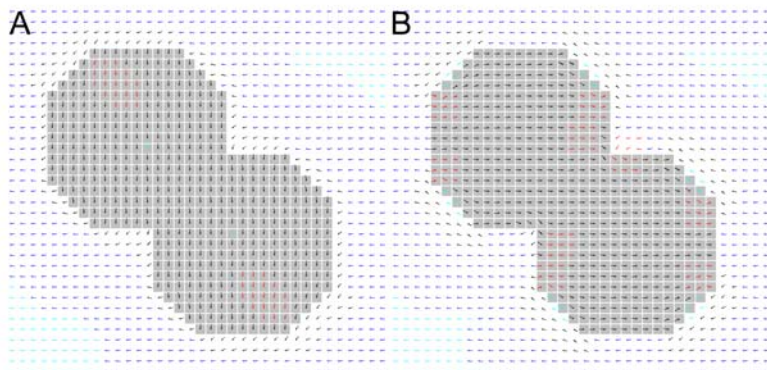


740

741

Accepted manuscript

741 Figure S6:



742

Accepted manuscript